Bio-based materials from sunflower co-products, a way to generate economical value with low environmental footprint

Philippe Evon, Landry Jégat, Laurent Labonne, Thierry Véronèse, Stéphane Ballas, Lucas Tricoulet, Jing Li, Danny Geelen

OCL 2023, 30, 25

https://doi.org/10.1051/ocl/2023028

OCL Oilseeds & fats Crops and Lipids

Available online at:
www.ocl-journal.org

RESEARCH ARTICLE OPEN ACCESS

Bio-based materials from sunflower co-products, a way to generate economical value with low environmental footprint☆

Philippe Evon[1,*], Landry Jégat[1], Laurent Labonne[1], Thierry Véronèse[2], Stéphane Ballas[2], Lucas Tricoulet[2], Jing Li[3] and Danny Geelen[3]

[1] Laboratoire de Chimie Agro-industrielle, Université de Toulouse, INRAE, ENSIACET, France
[2] Ovalie Innovation, 2 Rue Marguerite Duras, 32000, Auch, France
[3] HortiCell, Department Plants and Crops, Faculty of Bioscience Eng., Ghent University, Belgium

Received 3 October 2023 – Accepted 13 November 2023

Abstract – Sunflower co-products (*i.e.*, stalks and heads) were recently used to create a value chain of sunflower biomass. On the one hand, bioactive ingredients extracted through twin-screw extrusion can be valorized as ecologically friendly agricultural products. On the other hand, in this study, the remaining solid, *i.e.*, the extrudate, was used for obtaining bio-based materials, generating economical value with low environmental footprint. It is processable into cohesive boards through hot pressing. According to NF EN 312, optimal board (37 MPa flexural strength, and 33% thickness swelling) containing 9.1% (w/w) sunflower proteins as binder can be used as a type P2 board, *i.e.*, for interior fittings (including furniture) in dry environments. For P3 and P4 types, a thickness swelling lower than 20% and 21%, respectively, will be required. The extrudate can be also separated into long fibers and fines. Long fibers can be compression molded into low-density insulation blocks (49 mW/m K thermal conductivity). Fines can be used as a filler for reinforcing (bio)plastics, *e.g.*, polypropylene and poly (lactic acid). These bio composites could be injected into pots or tutors for plants, or even extruded into window openings or exterior decking.

Keywords: Sunflower / cultivation co-products / twin-screw extrusion / bioactive ingredients / bio-based materials

Résumé – Matériaux biosourcés à partir de co-produits de tournesol, un moyen de générer une valeur économique avec une faible empreinte environnementale. Les co-produits du tournesol que sont les tiges et les capitules ont été récemment utilisés pour créer une chaîne de valeur de la biomasse du tournesol. D'une part, des ingrédients bioactifs extraits par extrusion bi-vis peuvent être valorisés en tant que produits agricoles écologiques. D'autre part, dans cette étude, le solide restant qu'est l'extrudat a été utilisé pour obtenir des matériaux biosourcés, générant une valeur économique avec une faible empreinte environnementale. L'extrudat peut être transformé en panneaux cohésifs par pressage à chaud. Selon la norme NF EN 312, le panneau optimal (résistance à la flexion de 37 MPa et gonflement en épaisseur de 33%) contenant 9,1% (m/m) de protéines de tournesol comme liant peut être utilisé comme panneau de type P2, c'est-à-dire pour les aménagements intérieurs (y compris les meubles) dans des environnements secs. Pour les panneaux de types P3 et P4, un gonflement en épaisseur inférieur à 21% sera nécessaire. L'extrudat peut également être séparé en fibres longues et en fines. Les fibres longues peuvent être moulées par compression en blocs d'isolation de faible densité (conductivité thermique de 49 mW/m K). Les fines peuvent être utilisées comme charge pour renforcer les (bio) plastiques, par exemple le polypropylène et l'acide polylactique. Ces bio composites pourront être injectés en pots ou en tuteurs pour les plantes, ou même extrudés en ouvertures de fenêtres ou en lattes de terrasses extérieures (decking).

Mots clés : Tournesol / co-produits de culture / extrusion bi-vis / ingrédients bioactifs / matériaux biosourcés

☆ Contribution to the Topical Issue: "Non-Food Uses Of Oil- And Protein- Crops / Usages Non Alimentaires des Oléoprotéagineux".

* Auteur correspondant : philippe.Evon@toulouse-inp.fr

Highlight

- Cultivation co-products can create a value chain of sunflower biomass.
- Bioactive ingredients extracted through extrusion were used as ecologically friendly agricultural products.
- Formaldehyde-free fiberboards, insulation blocks or biocomposites are molded from extrudate.
- It generates economical value with low environmental footprint.

1 Introduction

Continued population growth and steady depletion of forest and fossil fuel resources have given rise to real concerns over the last 20 yr, resulting in the introduction of new environmental regulations. There has been considerable interest in the use of agricultural by-products or those derived from a first agro-industrial processing. Naturally rich in cellulose or lignocellulose, they are particularly interesting for applications in the field of bio-sourced composite materials, and constitute alternative sources of fibers that could be competitive with those found in current materials. Abundant and cheap, plant fibers have very little impact on the environment and do not compete with the food industry for land use (Uitterhaegen *et al.*, 2017). Above all, they save on the use of fossil resources. Inside composite materials, it is often their natural capacity for thermal insulation and/or their ability to mechanically reinforce thermoplastic matrices that are expected.

Recent research in the field of natural fiber-reinforced composites involve numerous molding techniques: single- and twin-screw extrusion, injection-molding, hot pressing, cold compression, 3D printing, etc. (Evon, 2021, 2023). Mechanical (Velásquez *et al.*, 2002; Okuda and Sato, 2004; Uitterhaegen *et al.*, 2017; Evon *et al.*, 2021a), thermal (Anglès *et al.*, 1999, 2001; Velásquez *et al.*, 2003; Xu *et al.*, 2006, Quintana *et al.*, 2009) and/or chemical treatments, and fiber surface modifications (Khalid *et al.*, 2021) are solutions often considered to improve the performance of plant fibers. These treatments increase fineness of fiber bundles and promote fiber individualisation (Anglès *et al.*, 1999; Xu *et al.*, 2006; Uitterhaegen *et al.*, 2017), modify the matrix-to-fiber interface inside composites (Pintiaux *et al.*, 2015; Khalid *et al.*, 2021), increase their dimensional stability (Quintana *et al.*, 2009), or reduce their water absorption (Anglès *et al.*, 2001; Velásquez *et al.*, 2003). They also help to composite manufacture as the increased accessibility of lignins and the formation of reactive monomer compounds following these treatments contribute to self-bonding during molding (Amalia Kartika *et al.*, 2016; Tajuddin *et al.*, 2016).

Many natural fibers can be used to manufacture such composite materials, *e.g.*, miscanthus (Velásquez *et al.*, 2003), kenaf core (Okuda and Sato, 2006), wheat straw (Halvarsoon *et al.*, 2009), banana bunch (Quintana *et al.*, 2009), oil palm trunk (Hashim *et al.*, 2011), sugarcane bagasse (Nonaka *et al.*, 2013), coriander straw (Uitterhaegen *et al.*, 2017), linseed flax (Khan *et al.*, 2021), kapok (Lyu *et al.*, 2021), hemp (Laqraa *et al.*, 2021), etc. Given their use properties, these materials could find applications in many fields, such as agriculture, ecological engineering, construction, load-bearing composites, packaging, paper industry, etc. (Evon, 2021, 2023). When plant fibers are incorporated into plastic matrices of renewable origin, 100% bio-based thermoplastic composites with a controlled end-of-life can be developed (Gamon *et al.*, 2013; Gautreau *et al.*, 2021; Laqraa *et al.*, 2021). Conversely, the incorporation of plant fibers into fossil-based plastic matrices will enable more durable use over time of the composites (Uitterhaegen *et al.*, 2018a).

In the specific case of fiberboard manufacture, the use of synthetic resins that are often toxic and dangerous has given rise to real concerns about the environment, human health and safety. This is particularly true of formaldehyde-based resins, which are widely used in wood-based panels. Indoor use of these panels can generate toxic formaldehyde emissions (Salthammer *et al.*, 2010). In addition, synthetic adhesives are relatively expensive, accounting for up to 30% of the total production cost (Van Dam *et al.*, 2004a). The production of binderless panels (Tajuddin *et al.*, 2016) or the use of natural binders such as lignins (Theng *et al.*, 2019), starch (Evon *et al.*, 2021b) or proteins (Evon *et al.*, 2015a) avoid the use of such chemical additives.

Sunflower co-products have already shown their interest in obtaining bio-based composite materials, including stem bark fibers for their mechanical reinforcement (Evon *et al.*, 2015a), pith for its thermal insulation (Verdier *et al.*, 2020; Laborel-Préneron *et al.*, 2022), or proteins from the seeds for their adhesive (Evon *et al.*, 2015a) and thermoplastic (Rouilly *et al.*, 2006) properties. In Evon *et al.* (2015b), twin-screw extrusion is presented as a new perspective for the biorefinery of sunflower whole plant. In addition to the aqueous extraction of oil from seeds in the form of oil-in-water emulsions that can be used in cosmetics, the use of the cake in the materials sector was also investigated. As it takes the form of a natural composite combining plasticized proteins used as green adhesive and fibers, three families of sunflower panels have been developed. High-density panels, which are self-bonded by the proteins, are the result of hot pressing the cake, and can be used as load bearing boards in a dry environment (Evon *et al.*, 2015a). Molded respectively hot under low pressure or cold with a starch-based binder, medium-density (Evon *et al.*, 2014a) or low-density (Evon *et al.*, 2015c) panels have also been obtained. They can be used to thermally insulate buildings.

Very recently, BioSUNmulant project (European Union, FACCE SURPLUS, 2020–2023) aimed to create an integrated value chain of sunflower biomass. Bioactive ingredients were extracted continuously from sunflower co-products (*i.e.*, stalks and heads) through twin-screw extrusion (Li *et al.*, under review). They are expected to be valorized as innovative and ecologically friendly agricultural products. In particular, the use of the sunflower extracts (SE) as biostimulatory products was recently evidenced (Li *et al.*, 2022). Antioxidant agents, *e.g.*, polyphenols, carbohydrates, proteins, etc., detected in SE may have contributed to this bioactivity. With a view to recycling the remaining solid leaving at the same time the twin-screw extruder, and as it contains both natural fibers and some proteins, it would seem sensible to use it to manufacture new generations of bio-based materials, which could generate

economic value while reducing the environmental footprint of the materials sector.

The aim of this study will be to consider the manufacture of three types of materials from this remaining solid, *i.e.*, fiberboards (with or without the addition of exogenous natural binder), thermal insulation for construction, and thermoplastic (bio)composites, whether derived from a matrix of fossil or bio-based origin.

2 Materials and methods

2.1 Materials

Sunflower raw material used in this study was the remaining solid (RS) generated simultaneously with the extraction of biostimulatory molecules from sunflower co-products, under the optimal operating conditions described in Li *et al.* (under review). With 96% (w/w) protein purity, sunflower protein isolate (SPI) used as an exogenous natural binder in fiberboards was obtained from an industrial cake according to the methodology described in Orliac *et al.* (2003). With 85% (w/w) starch content, the starchy binder used for the production of the low-density insulation blocks, reference number 28474, was obtained from Bostik (Colombes, France). Polypropylene (PP), type PPC 3660, was obtained from TotalEnergies (Feluy, Belgium). Poly (lactic acid) (PLA), type Ingeo™ Biopolymer 3251D, was obtained from NatureWorks LLC (Minnetonka, MN, USA). Maleic anhydride-grafted polypropylene (PP-g-MA) used as coupling agent for the PP-based biocomposites, type Licocene PP MA 6452 fine grain, was obtained from Clariant (Muttenz, Switzerland). Triethyl citrate (TEC), type DUB CTE, used as coupling agent for the PLA-based biocomposites was obtained from Stéarinerie Dubois (Ciron, France). Linseed oil, type N460501C14-A, and its hardener, type N480519C23-D, and commercial varnish for wood protection, type H904, used for the coating post-treatments of optimal fiberboard were obtained from Ardéa (Roche-lez-Beaupré, France) and V33 (Domblans, France), respectively.

2.2 Analytical methods

NF V 03-922, 03-908, and 18-100 French standards were used to determine the mineral, lipid, and protein contents, respectively. ADF-NDF (ADF, Acid Detergent Fiber; NDF, Neutral Detergent Fiber) method of Van Soest and Wine was used to estimate the three parietal constituents, *i.e.*, cellulose, hemicelluloses, and lignins (Van Soest and Wine, 1967, 1968). Measuring the mass loss of the test sample after 1 h in boiling water made it possible to determine the content in water-soluble components. Determinations were all carried out in triplicate.

2.3 Physical characterization of RS

A Shimadzu TGA-50 (Japan) analyser was used for the thermogravimetric analysis (TGA) of RS. A rate of 5 °C/min, from 25 to 750 °C, was used, and dynamic analysis was conducted in air. The test sample mass was about 10 mg. During analysis, the determination of sample mass was made at various temperatures. These data were then used to plot the percentage of undegraded sample (1 − D) (%) as a function of temperature, where:

$$D = \frac{W_o - W}{W_o}, \quad (1)$$

and W_0 and W are the weights at the starting point and during scanning (mg). Measurements were carried out in duplicate.

A 2 L test tube was used to determine apparent density of RS. Once filled, the tube was weighed in order to determine it. Tapped density of RS was obtained from a Granuloshop (Chatou, France) Densitap ETD-20 volumenometer. All determinations were carried out in triplicate.

2.4 Dry fractionation of RS

Dry fractionation of RS was first carried out at lab scale using a 500 g test sample mass of RS, and a Retsch GmbH (Haan, Germany) AS 300 vibratory sieve shaker to determine particle size distribution. Sieve acceleration was $1.5 \times g$, and sieving time was 10 min. Then, dry fractionation was conducted continuously using a Ritec (Signes, France) 600 vibrating sieving machine fitted with a single grid of 1 mm square holes. Mechanical sieving was conducted at around 25 kg/h. This generated continuously two distinct fractions, *i.e.*, the bigger one made of big particles and long fibers (referred to as *"long fibers"*), and the smaller one made of small particles and fines (referred to as *"fines"*). The choice of a 1 mm grid was made in order to generate two fractions of roughly equal mass, with long fibers more suitable for thermal insulation, and fines for reinforcing plastics.

2.5 Hot pressing

Fiberboards were molded from RS through hot pressing. Before molding, RS was dried overnight in a ventilated oven at 60 °C up to 3-4% moisture content, which limited outgassing of water vapour at the end of molding. Molding was conducted using a 400 tons capacity Pinette Emidecau Industries (Chalon sur Saône, France) heated hydraulic press, and a 150 mm × 150 mm aluminium mold. Fiberboards were manufactured from 150 g RS, and different molding parameters were firstly tested to produce binderless boards (*i.e.*, without adding any exogenous binder). A total of eighteen binderless boards (FB1 to FB18) were produced during this first phase (Tab. 1). Secondly, once the optimum molding conditions have been identified, four additional boards (SPI1 to SPI4) were manufactured by adding SPI as exogenous natural binder to RS, in proportions varying from 4.8 to 28.6% (w/w) in the 150 g mixture of these two solid fractions, corresponding to SPI-to-RS ratios between 5 and 40% (w/w). A homogeneous mixture was obtained by manual mixing for 1 min. Fiberboards were then conditioned in a climatic chamber at 60% relative humidity (RH) and 25 °C until their weight stabilized. Once equilibrated, fiberboards were cut into test specimens having a 13 cm length and a 3 cm width before undergoing bending tests, and into 50 mm square test specimens before undergoing internal bond strength and water immersion tests.

Table 1. Hot pressing conditions used for binderless fiberboards from RS.

Fiberboard	Mold temperature (°C)	Applied pressure (MPa)	Molding time (min)
FB1	180	10	1
FB2	180	10	2
FB3	180	10	3
FB4	180	20	1
FB5	180	20	2
FB6	180	20	3
FB7	180	30	1
FB8	180	30	2
FB9	180	30	3
FB10	200	10	1
FB11	200	10	2
FB12	200	10	3
FB13	200	20	1
FB14	200	20	2
FB15	200	20	3
FB16	200	30	1
FB17	200	30	2
FB18	200	30	3

2.6 Post-treatments on optimal fiberboard

Two different post-treatments (*i.e.*, coating and cooking) were applied to optimal fiberboard to make it more water-resistant. Coating was made using linseed oil as a drying oil, completed with a hardener, or a commercial varnish sold for wood protection. These two waterproofing agents were applied uniformly to all six sides of the panel using a brush. A Nabertherm GmbH (Lilienthal, Germany) muffle furnace was used for the cooking (*i.e.*, thermal) post-treatment. It consisted of a temperature gradient of 25 to 220 °C at 7.5 °C/min, followed by 10 min at 220 °C.

2.7 Compression molding

Compression molding of insulation blocks was carried out according to the same protocol as in Uitterhaegen *et al.* (2020). The starchy binder was dissolved at room temperature in water for 10 min under stirring, in the following mass proportions: 1 part of starchy binder, and 7.9 parts of water (*i.e.*, 11.25% (w/w) binder concentration). Then, a homogeneous mixture of this glue with the long fibers from RS was obtained by mechanical mixing for 5 min. Based on previous results (Uitterhaegen *et al.*, 2020), the proportion of starchy binder was chosen equal to 15% (w/w) of the mass of long fibers. The mixture was molded for 30 s by cold compression in a 150 mm × 150 mm aluminium mold to obtain 5 cm thick blocks. Four different blocks were produced, with masses of long fibers equal to 73.2 (minimal), 97.4 (+33%), 121.5 (+66%) and 146.4 g (+100%), respectively (Tab. 2). Once molded, the blocks were dried at 60 °C until all water added for dissolution of the binder had been removed. To ensure optimal drying, the block was removed from the ventilated oven every 12 h, and weighed immediately. Its mass was then compared with its initial mass, *i.e.*, immediately after molding. The block was kept in the ventilated oven until the difference between these two masses exceeded the mass of water added at the moment of the preparation of the binder solution, corresponding in Table 2 to the difference in mass between the binder solution and the starchy binder (see the two rightmost columns of the table). The duration for drying depended on the density of the block (the more the density, the more the drying duration), and it was between 36 h and 72 h. Blocks were then conditioned in a climatic chamber at 60% RH and 25 °C. For each molding condition tested, the insulating block was made in duplicate.

2.8 Twin-screw extrusion compounding

Prior to compounding, fines from RS were ground more finely using an Electra (Poudenas, France) F3 hammer mill fitted with a 500 μm screen, and then dried overnight at 80 °C up to a moisture content less than 1%. PP and PLA composite blends were produced using a Clextral (France, Firminy) Evolum 25 co-rotating and co-penetrating twin-screw extruder (25 mm for screw diameter (D)) having ten consecutive modules (1 m for the total barrel length (L), *i.e.*, L/D equal to 40). The compounding protocol was the same as in Uitterhaegen *et al.* (2018a). In particular, screw profile was defined as follows:

- Introduction of PP or PLA in module 1.
- Melting of PP or PLA in module 4 thanks to the use of a series of bilobe paddles, and two series of reverse screw elements, all three joined together.
- Introduction of fines from RS using a side feeder at the level of module 5.
- Dispersion of the filler in the PP or PLA molten matrix using three successive zones of bilobe paddles in modules 6 to 8, with the second kneading block completed by reverse screw elements immediately after.
- Degassing implemented at the level of module 9, and die positioned immediately after module 10.

With PP, temperature profile of modules and the die at the end of the barrel was the following: 60 °C/170 °C/180 °C/190 °C/180 °C/175 °C/165 °C/165 °C/160 °C/160 °C/160 °C (die). With PLA, it was as follows: 60 °C/175 °C/190 °C/190 °C/180 °C/175 °C/165 °C/165 °C/160 °C/160 °C/160 °C (die). In order to maintain module 1 at its set temperature of 60 °C, it was fitted (as were the following modules) with an integrated cooling system. For PP and PLA composite blends, screw rotation speed (S_S, rpm) was set at 500 rpm and 400 rpm, respectively, and total feed rate (Q, kg/h) was always 10 kg/h, except for neat PP and neat PLA where it was 9.5 kg/h. The feeding rates of the matrix, fines and coupling agent were adjusted according to the produced formulation (Tabs. 3 and 4). As in Uitterhaegen *et al.* (2018a), PP-g-MA was added at the level of module 5 *via* the side feeder in the PP composite blends in a proportion equal to 10% (w/w) of the mass of fines. For PLA composite blends, based on the results of a recent confidential study, the addition of TEC was much higher, *i.e.*, in a proportion equal to 25% (w/w) of the mass of fines, and it was made also in module 5. Three distinct gravimetric feeders were used to control the inlet flow rates of the three solids (*i.e.*, the polymer matrix, fines from RS, and PP-g-MA for PP composite blends). In the case of the PLA ones, TEC

Table 2. Molding conditions used for low-density insulation blocks from long fibers.

Insulation block	Binder content (%)	Mass of long fibers from RS	Long fibers from RS (g)	Starchy binder (g)	Binder solution (g)
IB1	15	Minimal	73.2	11.0	97.8
IB2	15	+33%	97.4	14.6	129.8
IB3	15	+66%	121.5	18.2	161.8
IB4	15	+100%	146.4	22.0	195.6

was injected in its liquid form thanks to a previously calibrated piston pump.

Specific mechanical energy (SME, W h/kg) associated with the compounding experiment was calculated according to the following formula:

$$SME = \frac{U \times I \times \sqrt{3} \times \frac{T}{100} \times \frac{S_S}{S_{max}} \times COS\phi}{Q}, \quad (2)$$

Where:

U is the motor's operating voltage (U = 400 V), I the current feeding the motor (I = 57 A), T the motor torque (%), S_{max} the maximum speed of the rotating screws (S_{max} = 1,200 rpm), and cos ϕ the theoretical yield of the extruder motor (cos ϕ = 0.90).

2.9 Injection-molding

A Negri Bossi (Cologno Monzese, Italy) VE 160-720 injection press having 160 tons clamping force was used to form the PP and PLA composite blends through injection molding. After injection, both tensile and bending test specimens were obtained. With PP, the temperature profile along the plasticizing screw and the nozzle was 150 °C/170 °C/180 °C/130 °C (nozzle). With PLA, it was 170 °C/175 °C/175 °C/180 °C (nozzle). Shot building occurred over a 25 mm length, with a 150 rpm screw speed and a 5 bars counter pressure. Injection speed was set at 100 mm/s with a 2,000 bars pressure. A 1,600 kN clamping force was applied, and mold temperature was kept at 20 °C with PP, and at 30 °C with PLA. A 15 s cooling time was applied before demolding. Continuous production of test specimens was possible for all composite blends. Test specimens were then conditioned in a climatic chamber at 60% RH and 25 °C.

2.10 Physical characterization of bio-based materials

Bending test specimens (or the whole block in the specific case of insulation materials) were used to determine their density. Thickness and width were measured at three points, and length at two points, with a 0.01 mm resolution electronic digital sliding caliper. Thickness, width, and length mean values were recorded to calculate the specimen volume, and test specimens were all weighed to calculate their density. All analyses comprised four repetitions.

For fiberboards, bending properties and internal bond strength (for optimal fiberboard only) were conducted using ISO 16978:2003 and 16260:2016 standards, respectively. An Instron 33R 4204 (Norwood, MA, USA) universal testing system was used. All analyses comprised four repetitions. ISO 868:2003 standard was used to determine Shore D surface hardness with a Bareiss GmbH (Oberdischingen, Germany) durometer. All measurements were conducted through thirty-two repetitions.

Table 3. Composition (in weight) of PP composite blends.

Formulation	PP (%)	PP-g-MA (%)	Fines (%)
PP0[1]	100.0	0.0	0.0
PP1	94.5	0.5	5.0
PP2	89.0	1.0	10.0

[1] PP0, neat PP extruded before injection-molding.

For insulation blocks, a Neotim (Albi, France) FP2C thermal conductivimeter with a hot wire was used to determine their thermal conductivities at 25 °C and an accuracy of 5%. More details about the experimental procedure are in Uitterhaegen *et al.* (2020). Once thermal conductivity was determined, thermal resistance was calculated considering a 5 cm thickness for the block. Determinations were carried out in triplicate.

For composite blends, tensile and bending tests were conducted using ISO 527-4:1997 and 178:2010 standards, respectively, and the same universal testing system. All analyses comprised five repetitions. ISO 179-1:2010 standard was used to determine the Charpy impact properties from unnotched specimens with a Testwell Wolpert (Gennevilliers, France) 0–40 daN cm apparatus. All analyses comprised eight repetitions.

For all materials produced (excluding insulation blocks), ISO 16983:2003 standard was used to determine their thickness swelling (TS, %) and water absorption (WA, %) after 24 h immersion in water at ambient temperature. 50 mm × 50 mm test specimens were used for fiberboards. For composite blends, the bending test specimens were used. All determinations were carried out through four repetitions.

3 Results

RS was analysed in terms of its physico-chemical characteristics. Results are presented in Table 5. They were completed by its thermogravimetric analysis in Figure 1, and its particle size distribution in Figure 2. Results of sieving on a continuous semi-industrial equipment gave a mass distribution of fractions smaller and larger than 1 mm of 42% (w/w) and 54% (w/w), respectively. Physico-chemical characterization of the resulting long fibers and fines is also appearing in Table 5.

Table 4. Composition (in weight) of PLA composite blends.

Formulation	PLA (%)	TEC (%)	Fines (%)
PLA0[1]	100.0	0.0	0.0
PLA1	93.8	1.3	5.0
PLA2	87.5	2.5	10.0
PLA3	81.3	3.8	15.0
PLA4	75.0	5.0	20.0
PLA5	68.8	6.3	25.0

[1] PLA0, neat PLA extruded before injection-molding.

Table 5. Physico-chemical characterization of RS, and long fibers and fines from its dry fractionation.

Material	RS	Long fibers	Fines
Chemical composition (% of dry matter)			
Minerals	7.6 ± 0.4	7.1 ± 0.2	7.8 ± 0.3
Lipids	4.5 ± 0.1	n.d.	n.d.
Proteins	3.2 ± 0.1	n.d.	n.d.
Cellulose	42.5 ± 0.8	47.3 ± 0.1	46.3 ± 0.1
Hemicelluloses	9.1 ± 0.1	10.1 ± 0.3	4.1 ± 0.3
Lignins	11.9 ± 0.2	13.9 ± 0.1	15.1 ± 0.5
Water-solubles	8.1 ± 0.5	12.2 ± 0.4	9.6 ± 0.3
Densities (kg/m^3)			
Apparent density	62.3 ± 0.8	50.4 ± 1.1	65.0 ± 0.7
Tapped density	98.2 ± 1.1	65.0 ± 0.4	109.1 ± 1.5

n.d., non determined.

Characteristics of fiberboards from RS, without (FB1 to FB18) and with SPI (SPI1 to SPI4), are given in Table 6. In Table 7, characteristics of SPI2 optimal fiberboard are compared with values recommended for type P1 to P7 panels according to NF EN 312 French standard dedicated to the specifications for particleboards. More specifically, Table 8 presents its thickness swelling before and after the three waterproofing post-treatments investigated. Characteristics of insulation blocks are given in Table 9. Quality rating for cohesion and machinability of the IB1 to IB4 blocks was evaluated using an internal assessment method, and results are mentioned in this table. In Table 9, the insulating materials are also compared with four conventional insulating materials as well as two innovative bio-based materials recently developed at lab scale. In Table 10, motor torque, specific mechanical energy, and cost of twin-screw extrusion compounding of neat matrices, and PP and PLA composite blends are mentioned. Table 11 presents the characteristics of neat matrices (before and after extrusion), and those of the PP and PLA composite bends.

4 Discussion

4.1 Physico-chemical characterization of RS, and its dry fractionation into long fibers and fines

Chemical composition of RS logically reveals high lignocellulosic fiber content, mainly from the sunflower stem and, to a lesser extent, from the head, with cellulose, hemicelluloses and lignin contents of 42.5%, 9.1% and 11.9%, respectively, giving a plant fiber content of 63.5% (Tab. 5). Mineral content is 7.6%, which is common for agricultural or agro-industrial co-products. It is also worth noting the presence of a significant, although low, proportion of lipids and proteins, with contents of 4.5% and 3.2%, respectively. Some seeds must have been present in the raw material entering the twin-screw extruder, all of them probably not having been properly separated from the heads when harvested in the field. RS also contains 8.1% water-solubles, compared with the content of 21.1 ± 0.3% in field-harvested co-products. This significant reduction in water-solubles is explained by their partial extraction in twin-screw extruder (up to 64% (w/w) for the extraction yield), making it possible to obtain an aqueous extract rich in biostimulant molecules (Li *et al.*, 2022, under review). The chemical nature of these molecules has been exhaustively described in Li *et al.* (2022). These were soluble proteins, carbohydrates, and polyphenolic compounds (*e.g.*, hydroxycinnamic acids, flavonoids, diarylheptanoids, etc.). As a result of mechanical shear applied in the twin-screw extruder, RS takes the form of a "fluffy" material with a tapped density of only 98 kg/m^3. Its composite nature, which combines cellulose fibers with other biopolymers known to have adhesive properties, notably proteins, hemicelluloses and lignins, makes it a material of choice for obtaining fiberboards by hot pressing.

Results of thermogravimetric analysis of RS are shown in Figure 1. An initial mass loss of around 10% is observed at 100 °C, corresponding to the evaporation of water. Organic compounds are then thermally degraded in three successive stages. The first stage is the main one, taking place between 225 and 330 °C. Resulting in decomposition of around 59% of the sample mass, this thermal phenomenon corresponds to the degradation of water-soluble components, lipids, proteins and hemicelluloses, followed by that of cellulose (Hatakeyama and Hatakeyama, 2004; Evon *et al.*, 2014b; Hidayat *et al.*, 2014; Evon *et al.*, 2019). Located between 405 and 485 °C, the second degradation stage represents a 15% loss in sample weight. It corresponds essentially to the degradation of lignins (Hidayat *et al.*, 2014; Evon *et al.*, 2015a; Theng *et al.*, 2019), which is in line with lignin content reported in Table 5. The third and final stage, between 565 and 625 °C, is much less important as it represents only 9% of the initial sample mass. As the analysis was carried out in air atmosphere, it probably involves the oxidation of primary degradation products (Uitterhaegen *et al.*, 2016). At the end of analysis, residual mass of just under 7% corresponds to minerals in RS, which is in agreement with the content in Table 5. In view of these results, a mold temperature of 200 °C during hot pressing is perfectly feasible without any risk of thermal decomposition of RS constituents.

Semi-industrial sieving of RS generates a small fraction, made up of particles smaller than 1 mm, representing 42% (w/w) of the initial mixture, in perfect agreement with the results of analytical sieving (Fig. 2) for which 44.1% (w/w) of the particles were smaller than 1 mm. Containing 71.3% plant fibers, the fraction bigger than 1 mm is made up of large particles of bark as well as long fiber filaments initially contained within the bark (*i.e.*, in its inner part), with a 400 µm average diameter and a length of up to 4 cm. It has the form of a

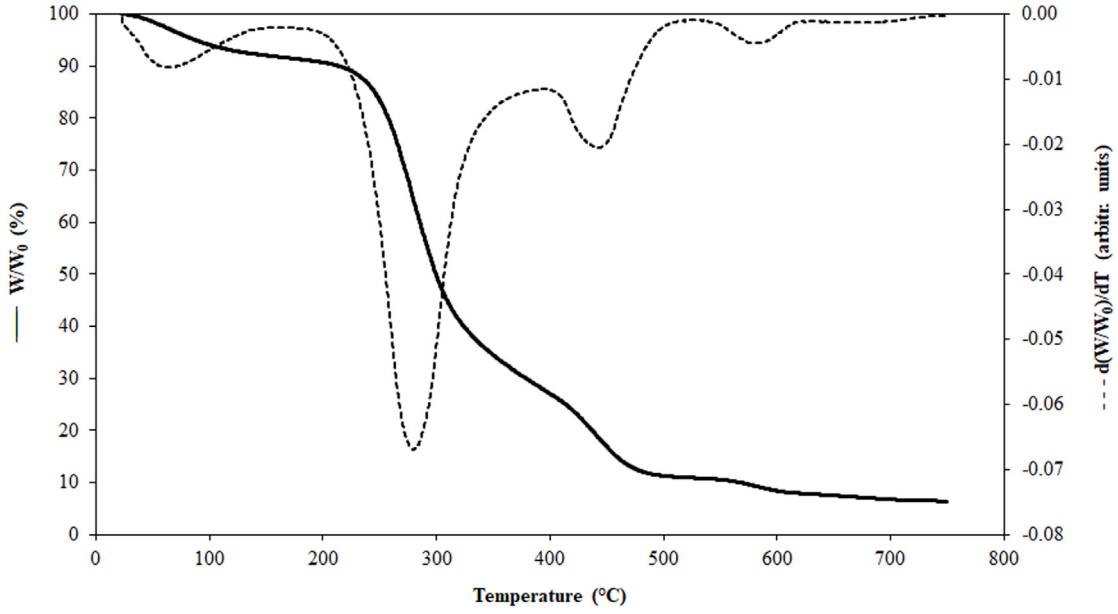

Fig. 1. TGA degradation curve of RS.

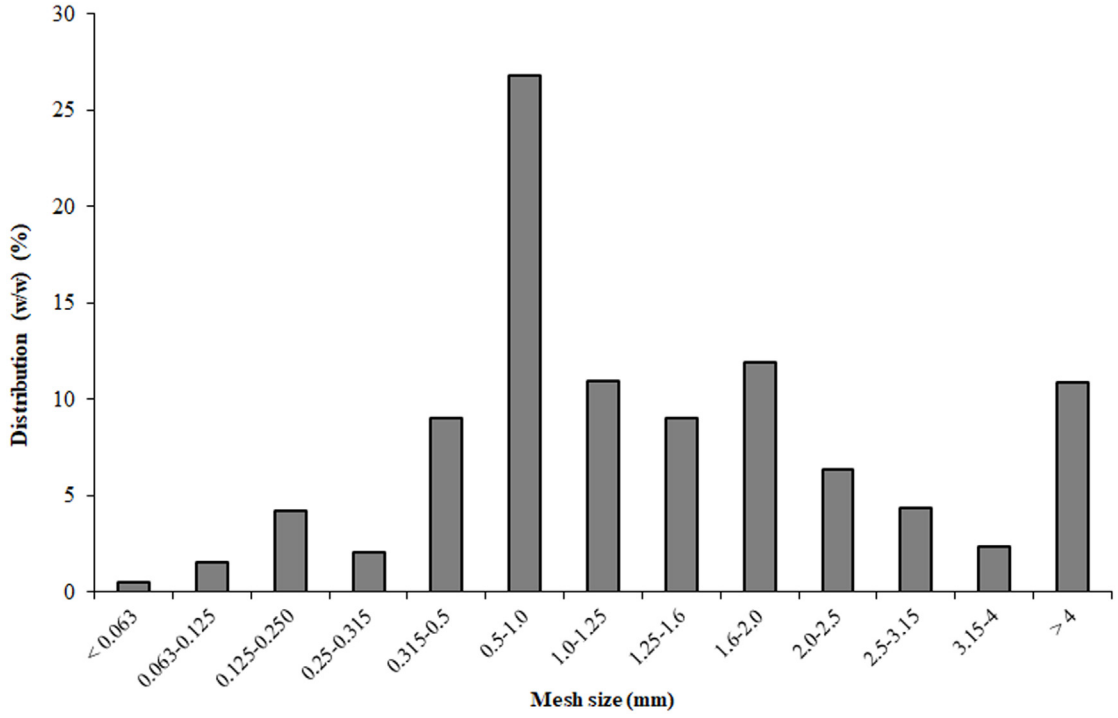

Fig. 2. Particle size distribution in RS.

Table 6. Characteristics of fiberboards produced from RS through hot pressing, without (FB1 to FB18) and with SPI (SPI1 to SPI4).

Fiberboard	Density (kg/m^3)	Flexural strength (MPa)	Elastic modulus (GPa)	Shore D (°)	TS (%)	WA (%)
FB1	934 ± 33	3.9 ± 0.5	0.4 ± 0.0	57.6 ± 2.6	n.m.	n.m.
FB2	1,055 ± 27	7.0 ± 0.8	0.9 ± 0.1	65.2 ± 0.8	n.m.	n.m.
FB3	1,091 ± 33	8.4 ± 0.7	1.1 ± 0.1	65.6 ± 1.9	n.m.	n.m.
FB4	1,154 ± 27	9.0 ± 1.0	1.1 ± 0.2	63.8 ± 0.8	n.m.	n.m.
FB5	1,185 ± 19	10.6 ± 1.1	1.4 ± 0.1	64.0 ± 0.7	n.m.	n.m.
FB6	1,206 ± 33	11.6 ± 1.2	1.6 ± 0.1	65.4 ± 0.7	n.m.	n.m.
FB7	1,234 ± 20	12.7 ± 0.9	1.6 ± 0.2	65.8 ± 1.4	n.m.	n.m.
FB8	1,236 ± 34	13.6 ± 1.2	1.7 ± 0.1	65.2 ± 1.9	n.m.	n.m.
FB9	1,275 ± 12	16.4 ± 0.7	2.3 ± 0.2	65.9 ± 1.1	470 ± 10	449 ± 10
FB10	820 ± 38	2.4 ± 0.1	0.3 ± 0.0	49.8 ± 0.6	n.m.	n.m.
FB11	899 ± 8	3.7 ± 0.5	0.4 ± 0.0	57.9 ± 0.9	n.m.	n.m.
FB12	970 ± 28	5.3 ± 0.4	0.7 ± 0.1	62.4 ± 0.9	n.m.	n.m.
FB13	1,131 ± 22	8.2 ± 0.4	0.9 ± 0.1	63.5 ± 0.7	n.m.	n.m.
FB14	1,204 ± 22	12.2 ± 1.3	1.3 ± 0.2	63.6 ± 1.5	n.m.	n.m.
FB15	1,242 ± 37	15.8 ± 0.9	2.0 ± 0.1	65.3 ± 0.8	391 ± 49	362 ± 25
FB16	1,252 ± 34	13.2 ± 1.1	1.6 ± 0.2	64.7 ± 0.8	n.m.	n.m.
FB17	1,274 ± 32	16.4 ± 1.2	2.1 ± 0.2	65.3 ± 1.0	410 ± 34	396 ± 15
FB18	1,304 ± 15	17.7 ± 1.7	2.3 ± 0.2	65.2 ± 1.7	306 ± 22	260 ± 22
SPI1[1,2]	1,267 ± 32	26.2 ± 0.7	3.3 ± 0.1	68.1 ± 1.2	192 ± 11	152 ± 8
SPI2[1,3]	1,270 ± 17	37.3 ± 0.7	4.6 ± 0.2	67.8 ± 1.3	169 ± 16	135 ± 8
SPI3[1,4]	1,234 ± 38	32.7 ± 1.1	4.1 ± 0.2	68.1 ± 1.3	137 ± 25	117 ± 9
SPI4[1,5]	1,152 ± 15	28.1 ± 1.2	2.8 ± 0.3	68.2 ± 1.1	84 ± 19	88 ± 2

n.m., non measurable (test specimens disintegrated, at least partially, after 24 h immersion).
[1] 200 °C mold temperature, 30 MPa applied pressure, and 3 min molding time for the hot-pressing conditions (i.e., those of FB18).
[2] 4.8% (w/w) for SPI in the solid mixture, corresponding to a SPI-to-RS ratio of 5% (w/w), or 7.7% total protein content in fiberboard.
[3] 9.1% (w/w) for SPI in the solid mixture, corresponding to a SPI-to-RS ratio of 10% (w/w), or 11.7% total protein content in fiberboard.
[4] 16.7% (w/w) for SPI in the solid mixture, corresponding to a SPI-to-RS ratio of 20% (w/w), or 18.7% total protein content in fiberboard.
[5] 28.6% (w/w) for SPI in the solid mixture, corresponding to a SPI-to-RS ratio of 40% (w/w), or 29.7% total protein content in fiberboard.

Table 7. Characteristics of SPI2 optimal fiberboard, and comparison with values recommended in NF EN 312.

Characteristic	SPI2	Type P1[1]	Type P2[2]	Type P3[3]	Type P4[4]	Type P5[5]	Type P6[6]	Type P7[7]
Flexural strength MPa)	37.3 ± 0.7	11.5 min	12.0 min	14.0 min	16.0 min	19.0 min	20.0 min	21.0 min
Elastic modulus (GPa)	4.6 ± 0.2	None	1.95 min	1.95 min	2.20 min	2.45 min	2.90 min	3.10 min
Internal bond strength (MPa)	0.85 ± 0.02	0.31 min	0.45 min	0.50 min	0.45 min	0.45 min	0.65 min	0.75 min
TS (%)	169 ± 16	None	None	20 max	21 max	14 max	16 max	10 max

[1] Panels for general use in dry environments.
[2] Panels for interior fittings (including furniture) used in dry environments.
[3] Non-working panels used in humid environments.
[4] Load bearing panels for use in dry environments.
[5] Load bearing panels for use in humid environments.
[6] Panels used under high stress in dry environments.
[7] Panels used under high stress in humid environments.

low-density fraction, with a tapped density (65 kg/m^3) even lower than that of RS (Tab. 5). This makes it a material of choice for thermal insulation materials. Containing 65.5% plant fibers, the fraction smaller than 1 mm is made up of small particles of bark, and fines generated during the extraction of bioactive molecules through extrusion, derived from the head, stem pith and seed residues. It has a much higher tapped density (109 kg/m^3). Its fineness makes it a material of choice for use as reinforcing filler in thermoplastics.

4.2 Characteristics of fiberboards produced from RS through hot pressing

Self-bonded fiberboards were first produced by direct hot pressing of RS using different conditions (Tab. 1). All boards are cohesive with characteristics in Table 6. This cohesion is explained by the contribution of hemicelluloses (Maréchal, 2001), proteins (Rouilly *et al.*, 2006; Evon *et al.*, 2015a), lignins (Van Dam *et al.*, 2004b; Domínguez-Robles *et al.*,

Table 8. Thickness swelling of SPI2 optimal fiberboard before and after waterproofing post-treatments.

Post-treatment	TS (%)
None	169 ± 16
Coating with linseed oil	123 ± 6 (−27%)
Coating with commercial varnish	118 ± 12 (−30%)
Cooking	33 ± 10 (−80%)

2017; Theng *et al.*, 2019) and, to a lesser extent, water-solubles to self-bonding.

At 3-4% moisture, hemicelluloses and proteins, which are amorphous biopolymers, have a glass transition temperature (T_g) of around 140–150 °C. At molding temperature of 180 °C min, they are necessarily in a viscous rubbery state, which contributes to fiber wetting. Lignins can also be used as a green adhesive, with high temperature and pressure necessary to mobilise the lignin-based binder (Tajuddin *et al.*, 2016). Once lignins are melted, a welding effect is generated at molding (Mason, 1928). Due to their high reactivity, they can be used as a bonding agent, whether steam explosion lignins (Van Dam *et al.*, 2004b), *Organosolv* lignins (Van Dam *et al.*, 2004b; Theng *et al.*, 2019) or Kraft lignins (Domínguez-Robles *et al.*, 2017).

In the present study, the higher the operating conditions, the denser the panels and the greater their mechanical strength (Fig. 3), as in Evon *et al.* (2015a). Applied pressure and molding time are the two operating variables with the greatest influence, while a mold temperature of 200 °C is favourable when pressure is 30 MPa. With increasingly severe conditions, hemicelluloses and proteins become more and more fluid in their viscous rubbery state, which improves fiber wetting and their adhesion to each other. Lignin mobilization as bonding agent is also exacerbated under these conditions. When measurable, water resistance of boards is very modest (306% min for TS). Surface hardness remains constant (62–68°) with the exception of FB1, FB10 and FB11, for which it is lower due to low pressure (10 MPa) and time (1 or 2 min) (Tab. 1).

Under best conditions (200 °C temperature, 30 MPa pressure, and 3 min time), *i.e.*, those of FB18, bending strength remains rather low (17.7 MPa) compared to a commercial MDF (20.7 MPa) (Simon *et al.*, 2020) and even a panel from sunflower whole plant biorefinery (30.3 MPa) (Evon *et al.*, 2015a), probably due to lower protein content (3.2% instead of 11.3%). It was therefore decided to add SPI to RS in order to increase the protein content in fiberboard. Extra proteins were added for both their thermoplastic and adhesive role. Fiber external surface is thus more wetted by the proteic binder, increasing mechanical strength of the panels while reducing their density, until optimal (complete) wetting by the proteins is achieved, at an SPI ratio of 9.1% (w/w) in the solid mixture, corresponding to a SPI-to-RS ratio of 10% (w/w), or 11.7% protein content in SPI2 (see footnote in Tab. 6). Such content is very close to that observed in the cake from sunflower whole plant (11.3%) used in Evon *et al.* (2015a). Beyond this content, a second, 100% protein phase is created inside board. Brittle in nature (Rouilly *et al.*, 2006), it weakens the board, leading to a reduction in bending properties for SPI3 and SPI4.

Optimal board (SPI2) exhibits a flexural strength of 37.3 MPa and an elastic modulus of 4.6 GPa, *i.e.*, +111% and +104%, respectively, than in optimal self-bonded board (FB18), showing the interest of adding SPI to RS. It is also less dense (−3%) and a little harder (+4%). Its flexural strength is higher than those of an older sunflower panel from whole plant and of a coriander one (30.3 MPa and 29.1 MPa, respectively) (Evon *et al.*, 2015a; Uitterhaegen *et al.*, 2017), but still lower than that of a panel based on extrusion-refined rice straw and Biolignin™ (50.3 MPa) (Theng *et al.*, 2019). Internal bond strength of SPI2 is also quite high, equal to 0.85 MPa (Tab. 7). As SPI2 was manufactured without adding formaldehyde-based resin, it will not emit formaldehyde, as it has recently been found for coriander board, also in the form of a composite blend of lignocellulosic fibers and proteins (Uitterhaegen *et al.*, 2018b; Simon *et al.*, 2020). This is a clear advantage of SPI2 for the environment, and human health.

Extraction of proteins contained in SPI under denaturing conditions makes them rather hydrophobic, which makes it possible to reduce TS as the proportion of SPI increases (up to 84% for SPI4 instead of 306% for FB18, *i.e.*, −73%). For SPI2, although reduced by 45%, TS is still high (169%) compared with recommendations of NF EN 312. Post-treatments were considered to make SPI2 even more water-resistant. The three post-treatments did reduce TS (Tab. 8). However, for the coating ones using hydrophobic liquids, reduction is relatively limited: −27% with linseed oil, and −30% with varnish. Thermal post-treatment shows the greatest efficiency, with TS decreasing from 169% to 33% (*i.e.*, −80%). Benefits of such treatment, frequently applied in industry to wood-based products to reduce hygroscopicity and increase dimensional stability, have already been demonstrated for injected sunflower cake (Rouilly *et al.*, 2006) and coriander boards (Uitterhaegen *et al.*, 2017). During thermal treatment, polymer chains become more mobile, and proteins and lignins more reactive (Rouilly *et al.*, 2006; Tjeerdsma *et al.*, 1998). Cross-linking reactions of hemicelluloses, lignins and proteins can occur, increasing SPI2 water resistance. It remains however to be seen whether such post-treatment will result in durable TS reduction over time.

In conclusion, with regard to NF EN 312, SPI2 is already usable as P1 (*i.e.*, panels for general use in dry environments) or P2 (*i.e.*, panels for interior fittings (including furniture) used in dry environments) type panels. From a mechanical point of view, it could even be used as P3 to P7 panels (Tab. 7). Nevertheless, and despite significant reduction in TS after cooking, the 33% value obtained remains too high for such uses. NF EN 312 recommends TS values of 20% max for type P3 (*i.e.*, non-working panels used in humid environments), 21% max for type P4 (*i.e.*, load bearing panels for use in dry environments), and even 10% max for type P7 (*i.e.*, panels used under high stress in humid environments).

For future work, and even though this would require cooling both press platens before opening to avoid uncontrolled outgassing of water vapour, it would be interesting to consider hot pressing with more water. Several studies have mentioned that adding more water improved lignin mobilization during hot pressing through plasticization (Orliac *et al.*, 2003; Xu *et al.*, 2006; Yamashita *et al.*, 2007, 2009; Takahashi *et al.*, 2010; Pintiaux *et al.*, 2015; Theng *et al.*, 2019). Excess water is also expected to act as a plasticizer for

Table 9. Characteristics of long fibers and low-density insulation blocks, and comparison with other insulating materials.

Material	Cohesion[1]	Machinability[1]	Density (kg/m^3)	Thermal conductivity (mW/m K)	Thermal resistance (m^2 K/W)[2]
Insulating materials from this study					
Long fibers in bulk	n.a.	n.a.	65.0 ± 0.4[3]	47.7 ± 0.2	1.05 ± 0.00
IB1	1	1	95.0 ± 3.0	n.d.	n.d.
IB2	2	2	107.4 ± 1.7	n.d.	n.d.
IB3	4	4	128.0 ± 0.3	48.8 ± 0.5	1.03 ± 0.01
IB4	4	4	134.5 ± 5.5	57.6 ± 0.7	0.87 ± 0.01
Conventional insulating materials (Laborel-Préneron *et al.*, 2022)					
Expanded polystyrene	n.a.	n.a.	20.0	32.0	1.56
Glass wool	n.a.	n.a.	27.5	35.0	1.43
Rock wool	n.a.	n.a.	35.0	38.0	1.32
Cellulose wadding	n.a.	n.a.	50.0	38.0	1.32
Innovative bio-based materials recently developed at lab scale					
Sunflower pith block (Verdier *et al.*, 2020)	5	5	43.0	39.0	1.28
Coriander straw block (Uitterhaegen *et al.*, 2020)	4	4	155.0	55.6	0.90

n.a., not applicable; n.d., non determined.
[1] Quality rating from 1 (min) to 5 (max).
[2] Thermal resistance for a 5 cm thick insulating material.
[3] This value corresponds to the tapped density.

hemicelluloses and proteins, reducing their glass transition temperatures (Rouilly *et al.*, 2006) and, as a result, lowering their melt viscosity. This in turn improves wetting of fiber external surface.

Similarly, to enable SPI2 to be used in humid conditions, its water resistance should be further improved, for example by coating with other bio-based solutions (*e.g.*, pine resin, vegetable waxes, hydrogenated vegetable oils, etc.). A lignin-based coating could also be considered. Even if one post-treatment would make it possible to reduce TS even further, it will be necessary to ensure that bending properties, and internal bond strength are maintained after prolonged contact with water.

4.3 Characteristics of low-density insulation blocks molded using long fibers from RS

Thermal conductivity of long fibers was first measured in bulk, at a density equal to their tapped density (65 kg/m^3), and it is 48 mW/m K (Tab. 9), not so far from that of cellulose wadding (38 mW/m K) (Laborel-Préneron *et al.*, 2022). Long fibers in bulk could therefore be used as loose thermal insulation. Insulation blocks were then manufactured by adding an amylaceous binder (binder with physical curing) as natural adhesive. For IB1, the mass of long fibers was calculated, from their tapped density, as the mass needed to fill a volume of 15 cm × 15 cm × 5 cm, *i.e.*, 73.2 g (Tab. 2). Next blocks (IB2 to IB4) were then manufactured by overestimating this mass by 33%, 66% and 100%, respectively, while maintaining the same proportion of starchy binder and retaining a 5 cm thickness after compression. Gradual increase in the density of the blocks was observed, the latter varying from 95 kg/m^3 for IB1 (higher than the tapped density of long fibers due to the addition of the binder) to 134 kg/m^3 for IB4 (Tab. 9).

Quality of the blocks in terms of cohesion and machinability was assessed qualitatively, and the two least dense blocks (*i.e.*, IB1 and IB2) were judged to be too fragile with regard to these criteria. For this reason, thermal conductivity was only measured on IB3 and IB4. Less dense than IB4, IB3 was the optimum material, being both a better insulator (49 mW/m K compared with 58 mW/m K for IB4) and resistant to machining. Although superior to various conventional insulating materials, of fossil (expanded polystyrene), mineral (glass wool, and rock wool) or vegetable (cellulose wadding) origin, IB3 has a thermal conductivity intermediate between those of two 100% bio-based materials, one from sunflower pith (39 mW/m K) and the other from extrusion-refined coriander straw (56 mW/m K) (Tab. 9). Molded from an inexpensive process that uses very low pressure (around 100 kPa) at room temperature, IB3 could find applications in the building sector. With a thickness of 5 cm, its thermal resistance is 1.0 m^2 K/W. For equivalent thermal resistance as that of expanded polystyrene (1.6 m^2 K/W), IB3 will still need to be thicker, *i.e.*, 7.6 cm instead of 5 cm (+51% in thickness).

Many tests still need to be carried out on optimum IB3 block. These include bending and compression tests, water resistance by determining the capillary water absorption coefficient, water vapour permeability, sound absorption properties, fire resistance, resistance to microbial growth, etc. In particular, IB3 is expected to have high water vapour permeability value, as for the vast majority of plant fiber-based insulating materials (Ratsimbazafy *et al.*, 2021). IB3 would therefore be a "breathable" material, which could ultimately

Table 10. Motor torque, specific mechanical energy, and cost of the twin-screw extrusion compounding of neat matrices, and PP and PLA composite blends.

Formulation	T (%)	SME (W h/kg)	Cost (c&z.euro;/kg)[1]
PP0	38.1 ± 0.5	593.9 ± 7.8	7.7 ± 0.1
PP1	38.9 ± 0.6	576.7 ± 8.4	7.5 ± 0.1
PP2	38.3 ± 0.5	567.2 ± 6.7	7.4 ± 0.1
PLA0	22.1 ± 0.3	275.1 ± 4.0	3.6 ± 0.1
PLA1	22.5 ± 0.4	266.1 ± 4.1	3.5 ± 0.1
PLA2	22.5 ± 0.4	266.2 ± 5.0	3.5 ± 0.1
PLA3	22.8 ± 0.5	270.5 ± 6.2	3.5 ± 0.1
PLA4	22.9 ± 0.7	270.9 ± 8.1	3.5 ± 0.1
PLA5	22.8 ± 1.1	269.9 ± 12.4	3.5 ± 0.2

[1] The electricity price in France in 2022 was 0.13 €/kW h.

contribute to improving living comfort in home. IB3's thermal conductivity will also have to be measured using the guarded hot plate method, *i.e.*, the more conventional one for measuring thermal conductivities of insulating materials. Determining its sound absorption properties will provide additional characterization. Thermal and sound insulation often go hand in hand, as recently observed with a sunflower pith material (Verdier *et al.*, 2020; Gomez-Campos *et al.*, 2023). Optimizations of the molding process should also be considered. These include optimizing the binder ratio and the nature of the binder, in particular by considering amylose-rich starches such as pea in order to achieve less sensitivity to water, or other binders such as chitosan which, in addition to its adhesive properties, also has interesting antimicrobial properties (Mati-Baouche *et al.*, 2014a, 2014b; Laborel-Préneron *et al.*, 2022).

4.4 Characteristics of PP-based and PLA-based biocomposites reinforced with fines from RS

Fines were used as reinforcing filler in PP (a non-biodegradable fossil polymer) and PLA (a bio-sourced polymer that biodegrades under controlled industrial composting conditions). Table 10 gives the production data in twin-screw extruder. Motor torque is independent of the filler content for the two plastic matrices. As the extruder's filling coefficient was the same whatever the filler content, this logically translates into stable specific mechanical energy, and thus compounding cost. Standard deviations associated with the motor torque are low (5% max of the mean value), reflecting stable operation during compounding. Much higher motor torque values are observed with PP (38–39% instead of 22–23% for PLA). Consequently, cost of compounding for PP composite blends is more than double: 7.5 c€/kg instead of 3.5 c€/kg. This is due to much higher viscosity of PP in its molten state. According to technical data sheets, PP has a melt flow index (MFI) of just 1.3 g/10 min at 230 °C and under 2.16 kg, compared with 30–40 g/10 min at 190 °C and up to 70–85 g/10 min at 210 °C for PLA. PP grade used here proved to be unsuitable due to excessive rheology. It rose initially through the degassing trunk in module 9. Before sampling, temperature profile in modules 9 and 10, and in the die had thus to be increased by 5 °C (*i.e.*, 160 °C instead of 155 °C), and screw rotation speed was also increased to apply higher mechanical shear (*i.e.*, 500 rpm instead of 400 rpm with PLA). Another alternative would have been to modify the screw profile, in particular to increase the shearing forces and at the same time to take advantage of the energy generated to avoid heating the last two modules and the die. Nevertheless, the decision was made in this study to use a single screw profile for the two polymer matrices tested (PP and PLA), for the purposes of comparison between the two polymers.

Despite this adaptation of both temperature profile and screw rotation speed, degradation of the reinforcing filler occurred with PP, illustrated by a slight smell of burning at the die exit, which was not observed with PLA even though temperature at the barrel end, and in the die was the same (160 °C). Because of the higher rheology of PP and its blends, for same filler content, residence time of the composite mixture is therefore longer than with PLA, resulting in partial thermal decomposition of the plant filler. From 10% (w/w) filler content, the rod surface is very rough due to this degradation. Rod also becomes very fragile. It was therefore decided not to go beyond this filler content. For PLA, which is much more fluid, no thermal decomposition occurred, making it easy to achieve a 25% (w/w) filler content. Above, rod at the die exit becomes very fragile and TEC even seems to evaporate, at least in part. It was therefore not possible to collect granules under these conditions.

Table 11 gives the characteristics of the composites, as well as those of the matrices, whether or not extruded before injection-molding. Here, extrusion of the matrices prior to injection was carried out to assess its effect on any deterioration in the properties of the plastic matrix itself. While no significant deterioration in characteristics of PP was observed (comparison between neat PP and PP0), the same was not true for PLA. When comparing neat PLA and PLA0, a significant decrease (−26%) in tensile and bending strengths was observed, without any negative effect on elastic moduli. This is probably the result of a screw profile that applies too mechanical shear to PLA, although suitable for PP, and which contributes to partial degradation in its strengths. In future, a single pair of reverse-pitch screws in the PLA melt zone would certainly be more suitable.

Table 11 also shows progressive increase with the filler content in the densities of the composites and their elastic moduli, both in tensile and bending, for both PP and PLA blends. Although small, the increase in densities can be

Table 11. Characteristics of neat matrices (before and after extrusion), and PP and PLA composite blends.

Formulation	Density (kg/m^3)	Tensile strength (MPa)	Young's modulus (GPa)	Flexural strength (MPa)	Elastic modulus (GPa)	Impact resilience (kJ/m^2)	TS (%)	WA (%)
Neat PP	837 ± 3	23.5 ± 0.3	1.1 ± 0.1	38.7 ± 0.6	1.0 ± 0.0	No rupture	0.2 ± 0.1	0.0 ± 0.0
PP0	839 ± 2	24.3 ± 0.4	1.3 ± 0.0	40.3 ± 0.5	1.0 ± 0.1	No rupture	0.1 ± 0.1	0.1 ± 0.0
PP1	849 ± 1	23.9 ± 0.4	1.5 ± 0.1	42.1 ± 1.5	1.1 ± 0.1	37.3 ± 3.9	0.3 ± 0.2	0.1 ± 0.0
PP2	862 ± 5	23.7 ± 0.5	1.5 ± 0.1	43.4 ± 1.0	1.3 ± 0.1	27.2 ± 1.9	0.9 ± 0.1	0.1 ± 0.0
Neat PLA	1,210 ± 5	59.2 ± 8.6	3.5 ± 0.1	73.1 ± 7.4	2.7 ± 0.4	11.7 ± 0.3	0.4 ± 0.2	0.0 ± 0.0
PLA0	1,217 ± 2	43.8 ± 3.2	3.6 ± 0.3	53.9 ± 5.3	2.9 ± 0.5	7.9 ± 0.5	0.3 ± 0.2	0.0 ± 0.0
PLA1	1,221 ± 5	38.0 ± 5.1	3.5 ± 0.2	51.9 ± 3.5	3.0 ± 0.4	5.2 ± 0.7	0.4 ± 0.1	0.1 ± 0.0
PLA2	1,229 ± 1	37.8 ± 3.1	3.8 ± 0.2	46.2 ± 4.0	3.1 ± 0.2	4.3 ± 0.8	0.4 ± 0.2	0.2 ± 0.1
PLA3	1,241 ± 4	36.0 ± 3.0	4.4 ± 0.4	41.6 ± 3.8	3.5 ± 0.2	3.9 ± 0.4	0.5 ± 0.1	0.4 ± 0.1
PLA4	1,249 ± 2	33.6 ± 4.7	4.6 ± 0.4	39.3 ± 3.7	3.6 ± 0.3	3.5 ± 0.3	0.7 ± 0.2	0.5 ± 0.1
PLA5	1,260 ± 3	32.6 ± 1.8	4.7 ± 0.4	32.4 ± 4.6	3.7 ± 0.3	3.2 ± 0.3	0.8 ± 0.2	1.2 ± 0.1

explained by the higher density of the filler itself (of the order of 1,350 kg/m^3) compared with those of the matrices (according to the data sheets, 905 kg/m^3 for PP and 1,240 kg/m^3 for PLA). The same was true with the incorporation into polypropylene or biopolyethylene of coriander straw in a flour form (Uitterhaegen *et al.*, 2018a). The increase in elastic moduli in the presence of a plant filler had also already been observed in PP with coriander flour (Uitterhaegen *et al.*, 2018a) or in PLA with bamboo and miscanthus fibers (Gamon *et al.*, 2013). This is explained by a gradual reduction in the mobility of the polymer chains when they are mixed with the filler, and confirms the suitability of RS fines for reinforcing the two plastic matrices tested. Stiffness of the composite blends thus increases as the plant filler content is increased, which inevitably leads to a progressive deterioration in impact resilience values. Impact resistance of PP composite blends is however much better than that of PLA-based ones (*e.g.*, at 10% (w/w) filler content, 27.2 kJ/m^2 for PP2 compared with only 4.3 kJ/m^2 for PLA2), and failure is not even reached for PP alone, whether or not extruded before injection. Better impact resilience of PP composite blends is the consequence of their lower stiffness.

The role of coupling agents was to reinforce the matrix-to-fiber interface. While PP-g-MA played its role well, enabling tensile strength of PP to be maintained and even slightly increasing bending strength (+8% for PP2 compared with PP0), the same cannot be said for TEC inside PLA blends. In these composites, tensile and bending strengths decrease progressively as the filler content increases: up to −26% and −40%, respectively, for PLA5 compared with PLA0, extruded before being injected. In a recent confidential study carried out in the laboratory on a PLA-based blend containing commercial wood flour as reinforcing filler, this bio-sourced additive proved its worth by keeping tensile and bending strengths stable as the level of wood flour in the blend increased. Tensile and bending strengths of PLA5 (32.6 MPa and 32.4 MPa, respectively) remain however relatively high, despite PLA degradation during compounding. Such biocomposite, filled with 25% (w/w) fines, has sufficient mechanical strength for one-off or ephemeral uses, such as plant pots or tutors. Biodegradable blends may be precisely of interest for such uses.

From the point of view of water resistance, TS and WA are always low (0.9% max and 1.2% max, respectively), even though they tend to increase slightly with the filling rate of fines (Tab. 11). It is therefore reasonable to assume that blends will have satisfactory water resistance during their use, including PLA ones despite their biodegradable nature. It is only when PLA blends come into contact with microorganisms in an industrial compost that their biodegradation will begin.

For future work, additional image analysis of the biocomposites, using, for example, scanning electron microscopy to observe the breaking patterns of tensile, flexural and/or impact test specimens, is likely to reveal more about the structure and organisation of these plastic composite materials (*e.g.*, fiber orientation, fiber-matrix interactions, etc.). For the same reasons, this image analysis could also be applied to fiberboards and low-density insulation blocks described above. Identifying a more fluid PP grade will also be necessary to limit thermal decomposition of plant filler. For example, polypropylene used in Uitterhaegen *et al.* (2018a), which has an MFI almost six times higher than that of the present study (7.5 g/10 min at 230 °C and under 2.16 kg), would be a possible alternative. This would probably make it possible to achieve higher filler contents, while limiting degradation of fines during compounding. At the same time, cost for raw materials would be reduced. RS has an estimated cost of 30 c€/kg, compared with around 1.50 €/kg for PP (and up to 2.50 €/kg for PLA). Non-biodegradable, these new PP composite blends will make good candidates for producing window openings or exterior decking, used over long periods and outdoors, replacing wood flour generally chosen for such applications. Similarly, for PLA composite blends, further study will be needed to adjust the proportion of TEC as morphology and chemical composition of RS fines are obviously different from those of wood flour, or even to consider another coupling agent. Replacing PLA with polyhydroxyalkanoates such as PHB (polyhydroxybutyrate), PHV (polyhydroxyvalerate), PHBV (polyhydroxy-co-butyrate-co-valerate), etc., would also be to consider. Like PLA, they are bio-based polyesters, but much more suitable for domestic or even soil composting, especially when filled with plant fibers.

Finally, with a view to intensifying the compounding process, it will be necessary to consider increasing the inlet

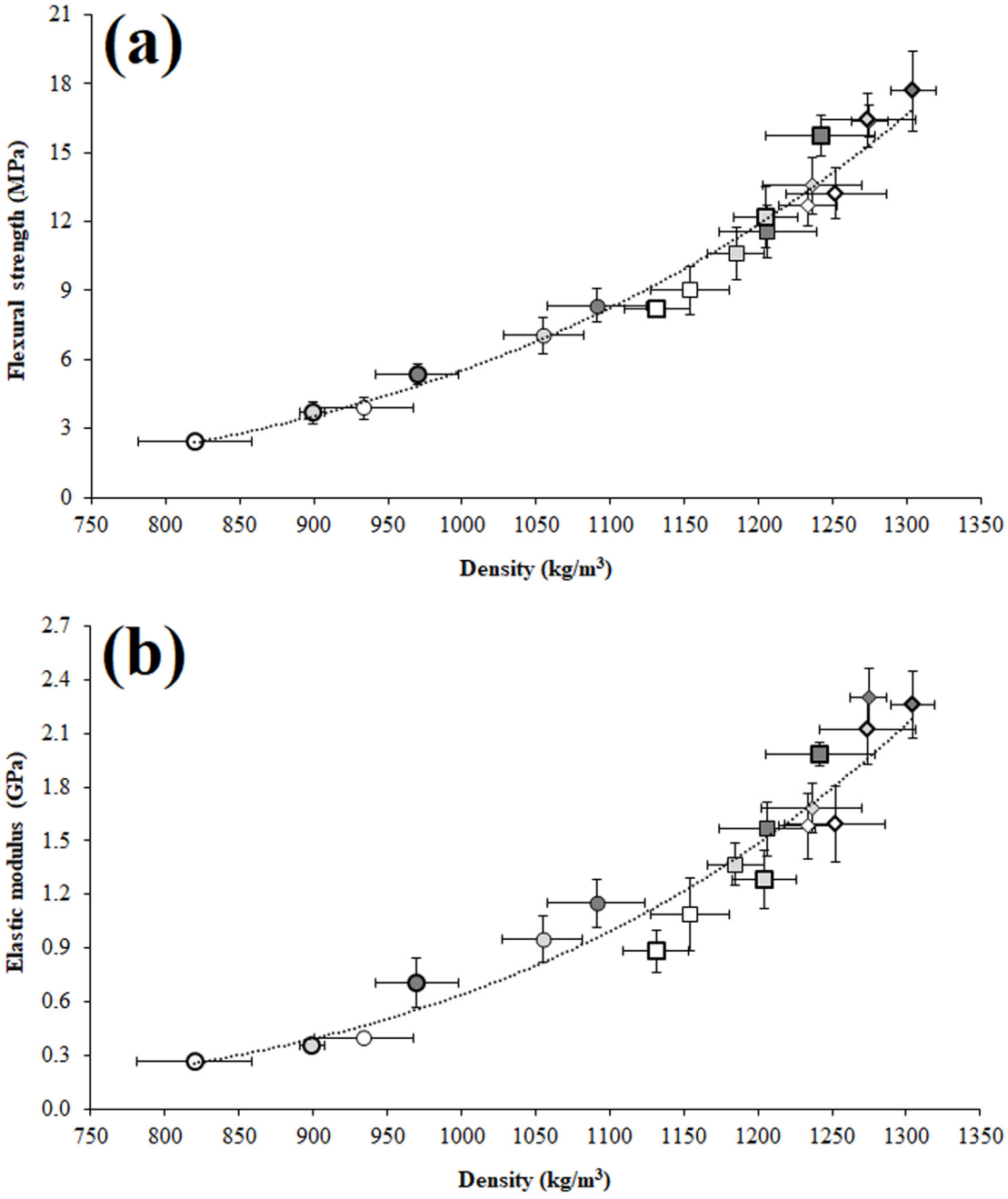

Fig. 3. Flexural strength (a) and elastic modulus (b) as functions of binderless fiberboard density. Symbols with thin and thick outlines correspond to mold temperatures of 180 and 200 °C, respectively. Round, square and trapezoid symbols correspond to applied pressures of 10, 20 and 30 MPa, respectively. Symbols with white, light grey and dark grey backgrounds correspond to molding times of 1, 2 and 3 min, respectively.

flow rates in Evolum 25. Based on results of this study and maximum screw rotation speed of this laboratory machine (1,200 rpm), inlet flow rates of the order of 25 kg/h can easily be achieved. In a second phase, compounding could be envisaged on an industrial-scale extruder. For example, with an Evolum 53 extruder (53 mm for screw diameter), *i.e.*, an entry-level industrial machine with a free volume almost 10 times greater than that of Evolum 25, inlet flow rates of around 250 kg/h should be achievable.

5 Conclusion

BioSUNmulant project has demonstrated that it is possible to extract molecules with biostimulant properties from the co-products of sunflower cultivation, *i.e.*, stalks and heads. During extraction conducted using the twin-screw extrusion technology, a residual solid, *i.e.*, the extrudate, is also generated. Essentially lignocellulosic in nature, this fraction is a raw material for obtaining bio-sourced materials.

In this study, fiberboards combining the residual solid with a sunflower protein isolate, used as an exogenous natural binder, were produced by hot pressing. They have promising mechanical properties, and could therefore be used in dry environments as a replacement for commercial wood-based panels, for example for interior fittings (including furniture). These boards do not emit formaldehyde, which is of real benefit to human health.

Residual solid was also fractionated into two distinct fractions using a semi-industrial sieving operation. Consisting of big bark particles and long fibers, the coarse fraction can be used to produce low-density insulation blocks with low thermal conductivity. These were obtained by compression molding in the presence of a starchy binder. They are a bio-based alternative to expanded polystyrene for the construction sector.

Made up of small bark particles and fines, the small fraction can be used to mechanically reinforce (bio)plastics such as polypropylene and poly (lactic acid). PLA-based composites, which are both 100% bio-sourced and biodegradable, could be used to make pots or tutors for plants, for example. At the same time, non-biodegradable PP-based composites could be used to produce window openings or exterior decking.

These three types of bio-based materials with low environmental footprint could provide an additional source of income for farmers, increasing the added value of sunflower cultivation. However, not all of these crop by-products should be used to avoid impoverishment of farm plots in organic matter.

Authors contributions

PE, and LL: conceptualization. PE: formal analysis. PE, and DG: funding acquisition. PE, LJ, and LL: investigation. PE, and LL: methodology. PE, and DG: project administration. PE, TV, SB, and LT: resources. PE, and DG: supervision. PE, and DG: validation. PE, and DG: visualization. PE: writing − original draft preparation. PE, JL, and DG: writing − review and editing. All authors contributed to the article and approved the submitted version.

Funding

This research was supported by European Union's Horizon 2020 Research and Innovation Program under a grant agreement for sustainable and resilient agriculture for food and non-food systems (project BioSUNmulant; FACCE SURPLUS, no. 652615), the Flanders Innovation and Entrepreneurship (VLAIO, Flanders) (no. HBC.2019.2244), and Agence Nationale de la Recherche (ANR) (no. ANR-20-FASU-0002-04, France).

Data Availability Statement

All data is contained within the article.

Acknowledgments

The authors thank all collaborating partners in the BioSUNmulant project. They would like to express their gratitude to Ovalie Innovation (Auch, France) for supplying the batch of the sunflower co-products used for the purpose of this study. They also thank sincerely M. Théo Prat-Dorgans and Ms. Nadia Zenasni, two student interns, for their significant contribution to the experimental work.

Declaration of conflict of interest

The authors declare no conflict of interest.

References

Amalia Kartika I, Evon Ph, Cerny M, *et al.* 2016. Simultaneous solvent extraction and transesterification of jatropha oil for biodiesel production, and potential application of the obtained cakes for binderless particleboard. *Fuel* 181: 870–877.

Anglès MN, Reguant J, Montané D, Ferrando F, Farriol X, Salvadó J. 1999. Binderless composites from pretreated residual softwood. *J Appl Polym Sci* 73: 2485–2491.

Anglès MN, Ferrando F, Farriol X, Salvadó J. 2001. Suitability of steam exploded residual softwood for the production of binderless panels. Effect of the pre-treatment severity and lignin addition. *Biomass Bioenergy* 21: 211–224.

Domínguez-Robles J, Tarrés Q, Delgado-Aguilar M, Rodríguez A, Espinach FX, Mutjé P. 2017. Approaching a new generation of fiberboards taking advantage of self lignin as green adhesive. *Int J Biol Macromol* 108: 927–935.

Evon Ph, Vandenbossche V, Pontalier PY, Rigal L. 2014a. New thermal insulation fiberboards from cake generated during biorefinery of sunflower whole plant in a twin-screw extruder. *Ind Crops Prod* 52: 354–362.

Evon Ph, Amalia Kartika I, Rigal L. 2014b. New renewable and biodegradable particleboards from jatropha press cakes. *J Renew Mater* 2: 52665.

Evon Ph, Vinet J, Labonne L, Rigal L. 2015a. Influence of thermo-pressing conditions on mechanical properties of biodegradable fiberboards made from a deoiled sunflower cake. *Ind Crops Prod* 65: 117–126.

Evon Ph, Vandenbossche V, Labonne L, Vinet J, Pontalier PY, Rigal L. 2015b. The thermo-mechano-chemical twin-screw reactor, a new perspective for the biorefinery of sunflower whole plant: aqueous extraction of oil and other biopolymers, and production of biodegradable fiberboards from solid raffinate. *OCL − Oilseeds fats Crops Lipids* 23: D505.

Evon Ph, Vinet J, Rigal M, Labonne L, Vandenbossche V, Rigal L. 2015c. New insulation fiberboards from sunflower cake with improved thermal and mechanical properties. *J Agric Stud* 3: 194–211.

Evon Ph, Barthod-Malat B, Grégoire M, *et al*. 2019. Production of fiberboards from shives collected after continuous fibre mechanical extraction from oleaginous flax. *J Nat Fibers* 16: 453–469.

Evon Ph. 2021. *Natural fiber based composites*, 1st ed. MDPI: Special Issue, Coatings, 11: 1031.

Evon Ph, Labonne L, Khan SU, Ouagne P, Pontalier PY, Rouilly A. 2021a. Twin-screw extrusion process to produce renewable fiberboards. *J Vis Exp e* 62072.

Evon Ph, de Langalerie G, Labonne L, *et al*. 2021b. Low-density insulation blocks and hardboards from amaranth (*Amaranthus cruentus*) stems, a new perspective for building applications. *Coatings* 11: 349.
Evon Ph. 2023. *Natural fiber based composites II*, 1st ed. MDPI: Special Issue, Coatings, 13: 1694.
Gamon G, Evon Ph, Rigal L. 2013. Twin-screw extrusion impact on natural fibre morphology and material properties in poly (lactic acid) based biocomposites. *Ind Crops Prod* 46: 173–185.
Gautreau M, Kervoelen A, Barteau G, *et al.* 2021. Fibre individualisation and mechanical properties of a flax-PLA non-woven composite following physical pre-treatments. *Coatings* 11: 846.
Gomez-Campos A, Sablayrolles C, Hamelin L, Rouilly A, Evon Ph, Vialle C. 2023. Towards fossil-carbon free buildings: Production and environmental performance of innovative sound absorbing panels made from sunflower straw. *J Clean Prod* 400: 136620.
Halvarsson S, Edlund H, Norgren M. 2009. Manufacture of non-resin wheat straw fibreboards. *Ind Crops Prod* 29: 437–445.
Hashim R, Said N, Lamaming J, *et al.* 2011. Influence of press temperature on the properties of binderless particleboard made from oil palm trunk. *Mater Des* 32: 2520–2525.
Hatakeyama T, Hatakeyama H. 2004. Thermal properties of green polymers and biocomposites. Dordrecht: Kluwer Academic Publishers.
Hidayat H, Keijsers ERP, Prijanto U, Van Dam JEG, Heeres HJ. 2014. Preparation and properties of binderless boards from *Jatropha curcas* L. seed cake. *Ind Crops Prod* 52: 245–254.
Khalid M, Imran R, Arif Z, *et al.* 2021. Developments in chemical treatments, manufacturing techniques and potential applications of natural-fibers-based biodegradable composites. *Coatings* 11: 293.
Khan SU, Labonne L, Ouagne P, Evon Ph. 2021. Continuous mechanical extraction of fibres from linseed flax straw for subsequent geotextile applications. *Coatings* 11: 852.
Laborel-Préneron A, Ampe C, Labonne L, Magniont C, Evon Ph. 2022. Thermal insulation blocks made of sunflower pith particles and polysaccharide-based binders: influence of binder type and content on their characteristics. *Constr Technol Archit* 1: 43–50.
Laqraa C, Ferreira M, Rashed Labanieh A, Soulat D. 2021. Elaboration by wrapping process and multiscale characterisation of thermoplastic bio-composite based on hemp/PA11 constituents. *Coatings* 11: 770.
Li J, Evon Ph, Ballas S, *et al.* 2022. Sunflower bark extract as a biostimulant suppresses reactive oxygen species in salt-stressed Arabidopsis. *Front Plant Sci* 13: 837441.
Li J, Khai Trinh H, Tricoulet L, *et al.* 2023. Under review. Biorefinery of sunflower by-products: optimization of twin-screw extrusion for novel biostimulants. *J Clean Prod* (submitted to journal July 7, 2023).
Lyu L, Zhang D, Tian Y, Zhou X. 2021. Sound-absorption performance and fractal dimension feature of kapok fibre/polycaprolactone composites. *Coatings* 11: 1000.
Maréchal P. 2001. Analyse des principaux facteurs impliqués dans le fractionnement combiné de pailles et de sons de blé en extrudeur bi-vis : obtention d'agromatériaux, Ph.D. tesis. France: INP, Toulouse.
Mason W. 1928. Process of making structural insulating boards of exploded lignocellulose fiber. Laurel: MF Company.
Mati-Baouche N, Elchinger PH, de Baynast H, Pierre G, Delattre C, Michaud P. 2014a. Chitosan as an adhesive. *Eur Polym J* 60: 198–212.
Mati-Baouche N, de Baynast H, Lebert A, *et al.* 2014b. Mechanical, thermal and acoustical characterizations of an insulating bio-based composite made from sunflower stalks particles and chitosan. *Ind Crops Prod* 58: 244–250.
Nonaka S, Umemura K, Kawai S. 2013. Characterization of bagasse binderless particleboard manufactured in high-temperature range. *J Wood Sci* 59: 50–56.
Okuda N, Sato M. 2004. Manufacture and mechanical properties of binderless boards from kenaf core. *J Wood Sci* 50: 53–61.
Okuda N, Sato M. 2006. Water resistance properties of kenaf core binderless boards. *J Wood Sci* 52: 422–428.
Orliac O, Rouilly A, Silvestre F, Rigal L. 2003. Effects of various plasticizers on the mechanical properties, water resistance and aging of thermo-moulded films made from sunflower proteins. *Ind Crops Prod* 18: 91–100.
Pintiaux T, Viet D, Vandenbossche V, Rigal L, Rouilly A. 2015. Binderless materials obtained by thermo-compressive processing of lignocellulosic fibers: a comprehensive review. *BioResources* 10: 1915–1963.
Quintana G, Velásquez J, Betancourt S, Gañán P. 2009. Binderless fiberboard from steam exploded banana bunch. *Ind Crops Prod* 29: 60–66.
Ratsimbazafy HH, Laborel-Préneron A, Magniont C, Evon Ph. 2021. A review of the multi-physical characteristics of plant aggregates and their effects on the properties of plant-based concretes. *Recent Prog Mater* 3: 69.
Rouilly A, Orliac O, Silvestre F, Rigal L. 2006. New natural injection-moldable composite material from sunflower oil cake. *Bioresour Technol* 97: 553–561.
Salthammer T, Mentese S, Marutzky R. 2010. Formaldehyde in the indoor environment. *Chem Rev* 110: 2536–2572.
Simon V, Uitterhaegen E, Robillard A, *et al.* 2020. VOC and carbonyl compound emissions of a fiberboard resulting from a coriander biorefinery: comparison with two commercial wood-based building materials. *Environ Sci Pollut Res* 27: 16121–16133.
Tajuddin M, Ahmad Z, Ismail H. 2016. A review of natural fibers and processing operations for the production of binderless boards. *BioResources* 11: 5600–5617.
Takahashi I, Sugimoto T, Takasu Y, Yamasaki M, Sasaki Y, Kikata Y. 2010. Preparation of thermoplastic molding from steamed japanese beech flour. *Holzforschung* 64: 229–234.
Theng D, Arbat G, Delgado-Aguilar M, *et al.* 2019. Production of fiberboards from rice straw thermo-mechanical extrudates using thermopressing: influence of fiber morphology, water addition and lignin content. *Eur J Wood Wood Prod* 77: 15–32.
Tjeerdsma BF, Boonstra M, Pizzi A, Tekely P, Militz H. 1998. Characterisation of thermally modified wood: Molecular reasons for wood performance improvement. *Holz Roh-Werkst* 56: 149.
Uitterhaegen E, Labonne L, Merah O, *et al.* 2016. Optimization of thermopressing conditions for the production of binderless boards from a coriander twin-screw extrusion cake. *J Appl Polym Sci* 134: 44650.
Uitterhaegen E, Labonne L, Merah O, *et al.* 2017. Impact of a thermomechanical fiber pre-treatment using twin-screw extrusion on the production and properties of renewable binderless coriander fiberboards. *Int J Mol Sci* 18: 1539.
Uitterhaegen E, Parinet J, Labonne L, *et al.* 2018a. Performance, durability and recycling of thermoplastic biocomposites reinforced with coriander straw. *Compos Part A Appl Sci Manuf* 113: 254–263.
Uitterhaegen E, Burianová K, Ballas S, *et al.* 2018b. Characterization of volatile organic compound emissions from self-bonded boards resulting from a coriander biorefinery. *Ind Crops Prod* 122: 57–65.
Uitterhaegen E, Labonne L, Merah O, *et al.* 2020. Innovative insulating materials from coriander (*Coriandrum sativum* L.) straw for building applications. *J Agric Stud* 8: https://doi.org/10.5296/jas.v8i4.17077.
Van Dam JEG, Van den Oever MJA, Keijsers ERP. 2004a. Production process for high density high performance binderless boards from whole coconut husk. *Ind Crops Prod* 20: 97–101.

Van Dam JEG, Van den Oever MJA, Teunissen W, Keijsers ERP, Peralta AG. 2004b. Process for production of high density/high performance binderless boards from whole coconut husk: Part 1: Lignin as intrinsic thermosetting binder resin. *Ind Crops Prod* 19: 207–216.

Van Soest PJ, Wine RH. 1967. Use of detergents in the analysis of fibrous feeds. IV. Determination of plant cell wall constituents. *J AOAC Int* 50: 50–55.

Van Soest PJ, Wine RH. 1968. Determination of lignin and cellulose in acid detergent fiber with permanganate. *J AOAC Int* 51: 780–785.

Velásquez JA, Ferrando F, Salvadó J. 2002. Binderless fiberboard from steam exploded miscanthus sinensis: The effect of a grinding process. *Holz Roh-Werkst* 60: 297–302.

Velásquez JA, Ferrando F, Farriol X, Salvadó J. 2003. Binderless fiberboard from steam exploded miscanthus sinensis. *Wood Sci Technol* 37: 269–278.

Verdier T, Balthazard L, Montibus M, Magniont C, Evon Ph, Bertron A. 2020. Using glycerol esters to prevent microbial growth on sunflower-based insulation panels. *Proc Inst Civ Eng: Constr.* https://doi.org/10.1680/jcoma.20.00002.

Xu J, Widyorini R, Yamauchi H, Kawai S. 2006. Development of binderless fiberboard from kenaf core. *J Wood Sci* 52: 236–243.

Yamashita O, Imanishi H, Kanayama K. 2007. Transfer molding of bamboo. *J Mater Process Technol* 192: 259–264.

Yamashita O, Yokochi H, Miki T, Kanayama K. 2009. The pliability of wood and its application to molding. *J Mater Process Technol* 209: 5239–5244.

Cite this article as: Evon P, Jégat L, Labonne L, Véronèse T, Ballas S, Tricoulet L, Li J, Geelen D. 2023. Bio-based materials from sunflower co-products, a way to generate economical value with low environmental footprint. *OCL* 30: 25.